Biophysical Journal, Volume 99

Supporting Material

Title: Mapping conformational ensembles of Abeta oligomers in molecular dynamics simulations

Seongwon Kim, Takako Takeda, and Dmitri Klimov

Supplemental Materials

Selection of truncated Aβ10-40 peptide

Several lines of evidence support similarities in Aβ1-40 and Aβ10-40 conformational ensembles. First, there is a good agreement between the experimental distribution of chemical shifts for Cα and Cβ atoms in Aβ1–40 monomers and the computed distribution of chemical shifts for the same atoms in Aβ10–40 monomers (ref. [28] from the paper, Fig. 7). Consistent with this observation, our previous simulations showed that the deletion of the N-terminal results in rather minor changes (< 20%) in Aβ monomer secondary structure (ref. [34] in the paper). Second, experiments and simulations (refs. [33,34] in the paper) suggest that the first nine N-terminal amino acids do not qualitatively affect the structures of Aβ oligomers, including their aggregation interface. For example, *in vitro* Aβ1-40 and Aβ10-40 peptides form continuous distributions of species from monomers to tetramers with small addition of peptamers (ref. [33] in the paper). Our previous simulations indicated that the location of the primary aggregation interface (residues 10-23) is not changed by the N-terminal truncation (ref. [34] in the paper). Third, according to solid-state NMR experiments Aβ10-40 and its full-length counterpart Aβ1-40 have similar two-fold symmetry fibril structures (refs. [17,32] in the paper). Moreover, Aβ1-40 fibrils were shown to seed the growth of Aβ10-40 fibrils (ref. [32] in the paper). Therefore, it appears that Aβ10-40 can be considered as an approximate model of the full-length Aβ1-40 peptide.

Testing the accuracy of implicit solvent model

The accuracy of CHARMM19+SASA force field for describing Aβ aggregation can be assessed by comparing simulation and experimental results. To this end, we list below several such checkpoints.

1. According to our previous studies CHARMM19+SASA force field accurately reproduces the experimental distribution of chemical shifts for Cα and Cβ atoms in Aβ monomers (refs. [28] in the paper).
2. In this paper (Table 1) we compare the secondary structure in Aβ monomers, dimers, tetramers, and fibrils obtained from experiments and simulations. The experimental fractions of residues in β-strand conformation in these species are 0.24, 0.39, 0.45, and 0.57, respectively. Our *in silico* values are in good agreement with the experimental ones being equal to 0.24, 0.37, 0.39, and 0.52.
3. The average energy of interpeptide HB in the CHARMM19+SASA force field (-1.2 kcal/mol) agrees well with the experimental estimate (ref. [47] in the paper).
4. Our REMD simulations of CHARMM19+SASA model suggested that upon deposition Aβ peptide adopts docked and locked states (ref. [42] in the paper). This result is consistent with the dock-lock mechanism proposed on the basis of experiments [1].

5. The REMD simulations of CHARMM19+SASA model showed that the Aβ locking and docking temperatures are 360 and 380K, respectively (ref. [42] in the paper). This high thermostability of Aβ fibril is consistent with the calorimetric experiments of Goto and coworkers, who measured the dissociation temperature of Aβ fibril to be ~373K [2].
6. In agreement with the experiments CHARMM19+SASA force field predicts enhanced amyloidogenic propensity for Asp23Tyr mutant (ref. [38] in the paper).
7. We checked the dependence of fibril elongation on the choice of SASA solvation parameters. Specifically, we compared Aβ fibril elongation thermodynamics using original SASA parameters and those developed by Urs Haberthur (implemented in c34b1 CHARMM release). We found that the numbers of hydrophobic side chain contacts and hydrogen bonds between Aβ peptides differ by about 1%. This test was reported in ref. [37] in the paper.
8. We have previously used different implicit solvent model, EEF1, to study the growth of Aβ fibril [3]. Both models, EEF1 and SASA, agree on four important points: (a) two types of bound states can be distinguished – docked (small fibril-like content) and locked (elevated fibril-like content); (b) there are large free energy barriers (> RT) between docked and locked states; (c) the affinities of the fibril edges are different; (d) the sequence region 10-23 appears to be the primary aggregation interface involved in fibril growth.

Therefore, CHARMM19+SASA model captures, at least semi-quantitatively, the mechanism of Aβ aggregation.

Cluster analysis of Aβ conformations

Conformational ensembles sampled by Aβ10-40 peptides in the oligomers or as monomeric species were probed using the cluster analysis. Because the complete account of this method can be found in previous studies [4-6], here we present its brief description. The cluster analysis was applied to equilibrated structures collected from REMD simulations at 360K. In all, we used 5067 conformations of Aβ monomers, 5898 conformations of Aβ peptides in the dimer, and 5240 conformations of Aβ peptides in the tetramer. The structures were collected with the period of 15 (monomer), 40 (dimer), and 100 (tetramer) REMD exchange attempts. Due to large REMD acceptance rate the structures were, on an average, separated by multiple replica exchanges. As a result they can be considered statistically independent. Aβ conformations were clustered based on the distribution of intrapeptide side chain contacts. To this end, a conformation k was represented by a vector $\boldsymbol{D}(k)$ with 435 binary components, each given by the element in the intrapeptide contact map $C_{in}(i,j)$. If the residues i and j ($j>i+1$) form a contact, then $C_{in}(i,j)=1$, and $C_{in}(i,j)=0$, otherwise. The vector $\boldsymbol{D}_{cl}$ representing a cluster is computed as an average of the vectors $\boldsymbol{D}(k)$, where k are the indices of conformations assigned to a cluster. The peptide conformational clusters were defined by the cut-off radius R_c, which is equal to the maximum Euclidian distance between a cluster and a structure. The values of R_c were 5.8 (monomer), 5.7 (dimer), and 5.4 (tetramer). The selected R_c are the minimal

values that result in the distribution of structurally distinct populated clusters, which taken together represent more than 80% of all conformations. A cluster is considered populated, if it encompasses more than 10% of all conformations. Clusters are assumed structurally distinct, if they hold different secondary structure distributions. We checked that changing the number of structures passed from REMD simulations to cluster analysis has no qualitative effect on the cluster distributions.

Aggregation interface in Aβ oligomers

In our previous studies we have reported that most of interpeptide interactions in the Aβ10-40 dimer are formed by the Nt region (ref. [34] in the paper). To check if similar distribution of interpeptide interactions holds for the tetramer, we computed the map of interpeptide side chain contacts $<C_t(i,j)>$ (Fig. S1). The contact map reveals that the distribution of interactions is skewed toward the Nt. Indeed, the number of contacts formed between the Nt regions $<C_t(Nt,Nt)>\approx 5.5$, whereas the Nt-Ct and especially Ct-Ct interactions are less frequent ($<C_t(Nt,Ct)>\approx 3.0$, $<C_t(Ct,Ct)>\approx 1.6$). The dimer aggregation interface is qualitatively similar, for which we have previously obtained $<C_d(Nt,Nt)>\approx 8.3$, $<C_t(Nt,Ct)>\approx 4.8$, and $<C_t(Ct,Ct)>\approx 2.3$ (Table 1 in ref. [34]). The Nt peptide terminal forms, on an average, $<C_t(Nt)>\approx 30.2$ contacts with other peptides in the tetramer, whereas the Ct is engaged in $<C_t(Ct)>\approx 14.9$ contacts (or 2.2 and 1.4 contacts per residue, respectively). For the dimer, $<C_d(Nt)>\approx 16.1$ and $<C_d(Ct)>\approx 8.6$ (or 1.2 and 0.8 contacts per residue, respectively) (ref. [34] in the paper).

It is known from the solid-state NMR experiments that Aβ peptides in the fibril form in-registry parallel β-sheets (ref. [17] in the paper). Because relatively few hydrogen bonds are formed in Aβ oligomers, we check if interpeptide side chain contacts follow parallel or antiparallel interaction pattern. To this end, we devised the following procedure. For each pair of interacting peptides in the tetramer we computed a contact map $C_t(i,j)$ and define two vectors p and a. If there is a contact between the residues i and j (i.e, $C_t(i,j)=1$), then $p(i+j)=1$ and $a(i-j)=1$. A given contact map is then represented by the pair of numbers Σ_p and Σ_a equal to the sum of non-zero elements of p and a, respectively. According to this mapping, a perfect parallel in-registry structure formed by two peptides (all main diagonal elements in $C_t(i,j)$ are non-zero) is represented by the values $\Sigma_p=31$ and $\Sigma_a=1$. (Note $N=31$ is the number of residues in Aβ.) If peptides form parallel off-registry aggregation interface, $\Sigma_p<31$, but Σ_a is still 1. A perfect antiparallel in-registry structure (all anti-diagonal elements in $C_t(i,j)$ are non-zero) is mapped to $\Sigma_p=1$ and $\Sigma_a=31$. If peptides form antiparallel off-registry aggregation interface, $\Sigma_a<31$, but $\Sigma_p=1$. However, if aggregation interface contains equal number of parallel and antiparallel contacts (in- or off-registry), $\Sigma_p=\Sigma_a$. Therefore, mapping the contact map onto the point (Σ_p,Σ_a) on a plane provides a convenient representation of the amount of parallel and antiparallel structure in Aβ oligomer. Using REMD simulations we computed the probability distribution $P(\Sigma_p,\Sigma_a)$ for the tetramer

(Fig. S2). The plot demonstrates that on an average a pair of Aβ peptides forms an aggregation interface with approximately equal number of parallel and antiparallel contacts. This result is consistent with the structure of Aβ oligomer, in which peptides have no preferential mutual orientation.

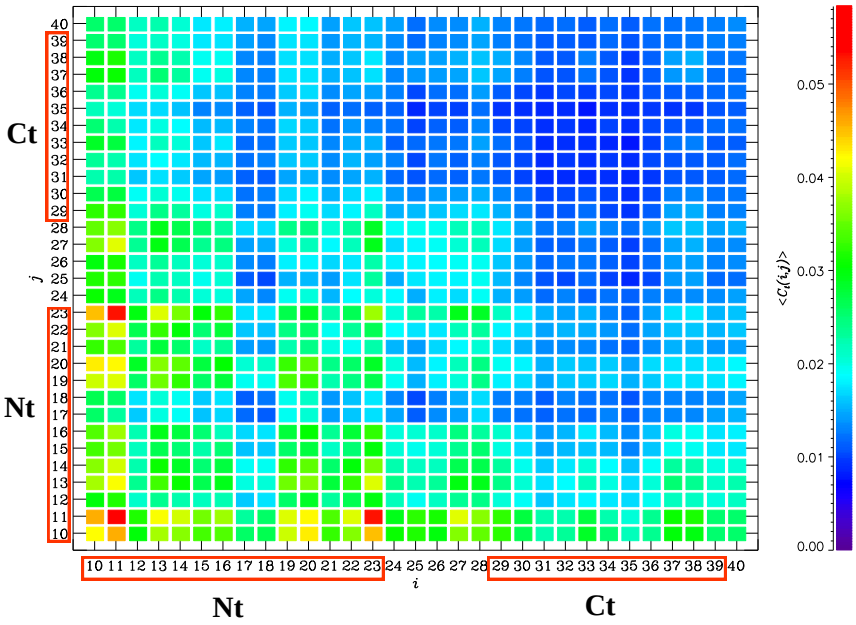

Figure S1 The contact map <$C_t(i,j)$> displays the probabilities of forming side chain contacts between a pair of Aβ peptides in the tetramer. The indices *i* and *j* represent the residues in Aβ peptides. The map <$C_t(i,j)$> is computed at 360K and color coded according to the scale. The residues from the Nt and Ct sequence regions are boxed. The plot suggests that the aggregation interface is largely confined to the Nt region.

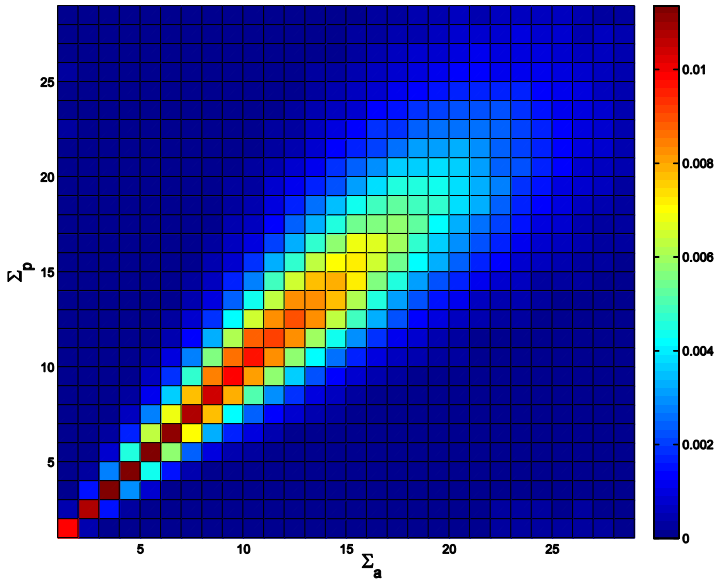

Figure S2 The probability distribution $P(\Sigma_p,\Sigma_a)$ of the measures of parallel and antiparallel interactions, Σ_p and Σ_a , in the tetramer aggregation interface. The probabilities $P(\Sigma_p,\Sigma_a)$ are computed at 360K and color coded according to the scale.

References:

1. Esler, W. P., E. R. Stimson, J. M. Jennings, H. V. Vinters, J. R. Ghilardi, J. P. Lee, P. W. Mantyh, and J. E. Maggio, 2000. Alzheimer's disease amyloid propagation by a template-dependent dock-lock mechanism. *Biochemistry* **39**: 6288-6295.
2. Sasahara, K., H. Naiki, and Y. Goto. 2005. Kinetically controlled thermal response of β2-microglobulin amyloid fibrils. *J. Mol. Biol.* **352**:700–711.
3. Takeda, T. and Klimov, D. K., 2008. Temperature induced dissociation of Aβ monomers from amyloid fibrils. *Biophys. J.* **95**:1758-1772.
4. Klimov, D.K. and D. Thirumalai, 2004. Progressing from folding trajectories to transition state ensemble in proteins. *Chem Phys* **307**:251–258.
5. Pao, Y.-H., 1989. Adaptive Pattern Recognition and Neural Networks, Addison-Welsley, New York.
6. Karpen, M. E., D. J. Tobins, and C. L. Brooks, III, 1993. Statistical clustering techniques for the analysis of long molecular dynamics trajectories: analysis of 2.2 ns trajectories of YPGDY. *Biochemistry* **32**:412-420.